Compression of hollow-circular fiber-reinforced rubber bearings

Seval Pinarbasi* and Fuad Okay

Department of Civil Engineering, Kocaeli University, Umuttepe Campus, 41380, Kocaeli, Turkey

Abstract. Earlier studies on hollow-circular rubber bearings, all of which are conducted for steel-reinforced bearings, indicate that the hole presence not only decreases the compression modulus of the bearing but also increases the maximum shear strain developing in the bearing due to compression, both of which are basic design parameters also for fiber-reinforced rubber bearings. This paper presents analytical solutions to the compression problem of hollow-circular fiber-reinforced rubber bearings. The problem is handled using the most-recent formulation of the "pressure method". The analytical solutions are, then, used to investigate the effects of reinforcement flexibility and hole presence on bearing's compression modulus and maximum shear strain in the bearing in view of four key parameters: (i) reinforcement extensibility, (ii) hole size, (iii) bearing's shape factor and (iv) rubber compressibility. It is shown that the compression stiffness of a hollow-circular fiber-reinforced bearing may decrease considerably as reinforcement flexibility and/or hole size increases particularly if the shape factor of the bearing is high and rubber compressibility is not negligible. Numerical studies also show that the existence of even a very small hole can increase the maximum shear strain in the bearing significantly, which has to be considered in the design of such annular bearings.

Keywords: rubber; elastomeric bearing; hollow-circular bearing; fiber-reinforced bearing; reinforcement flexibility; radius ratio; bulk compressibility; shape factor; compression modulus; seismic isolation.

1. Introduction

Due to its favorable mechanical properties, rubber has long been used in various engineering applications, such as isolation of bridges from thermal expansion or of buildings from earthquakes. In these applications, rubber components are usually designed to have low horizontal stiffness to isolate the structure from horizontal excitations, yet high vertical and bending stiffness to support the heavy weight of the superstructure (Kelly 1997). However, besides its low shear modulus, which ranges from $G = 0.30$ MPa to $G = 2.22$ MPa, rubber has very little compressibility, e.g., Poisson's ratio of natural rubber is $v \cong 0.4997$ (Lindley 1974). For this reason, a rubber block, if used in its "bulky" form, can*not* support a vertical load or a bending moment without making considerable deformations. This problem can easily be overcome by using rubber in its "bonded", or "reinforced", form, as in the case of steel-laminated multilayered rubber bearings, which are composed of several thin rubber layers interleaved by and bonded to steel shim plates. In fact, by

*Corresponding author, Assistant Professor, E-mail: sevalp@gmail.com

bonding the top and bottom faces of a soft rubber layer (with $G \cong 1$ MPa) to "rigid" surfaces (such as, steel plates which has $G \cong 80000$ MPa), "incompressibility" of rubber can be used in a *favorable* manner since, as stated by Lindley (1968), "for materials such as rubber which have a low shear modulus but a relatively high bulk modulus, any restrictions on their freedom to change shape can have a very marked effect on their stiffness in compression". Thus, it is possible to increase the vertical/bending stiffness of a "reinforced" rubber unit as much as required simply by changing the thickness of "bonded" rubber layers, in other words, by changing the amount of "constrained" rubber. This is, in fact, one of the main reasons for outstanding success of rubber in many engineering applications as spring/isolator for over a century.

In earlier engineering applications, rubber has mostly been used as bridge bearings, helicopter rotor bearings, wharf fenders and elastic foundations to machinery and motors. In the last two decades, the use of rubber has extended to earthquake resistant design applications. Many seismic isolated buildings and bridges with rubber-based isolation systems at their bases have been constructed, and continue being constructed, in all over the world (Naeim and Kelly 1999). Advances in computer technology leads to advanced analytical techniques for investigating seismic behavior of such isolated structures (e.g., Kim *et al.* 2008, Olmos and Roesset 2010). Similarly, advances in material science result in development of different innovative isolator types (Kelly 1997). Until recently, seismic isolation technique has almost entirely applied to large buildings with sensitive equipment and/or historical value and/or post-earthquake importance. The conventional rubber-based isolators used in these applications are usually considerably large, heavy and expensive due to the presence of steel shim plates as reinforcing elements. Kelly (1999, 2002) has conducted experimental and analytical studies to examine feasibility of using fiber reinforcement in place of steel sheets, which, if possible and feasible, can decrease both the cost and weight of the isolators, and verified that it is possible to produce a fiber-reinforced bearing that matches the behavior of its steel-reinforced counterpart. Although the idea is new, the viability of the concept has already been investigated and proven through several experimental and analytical studies (e.g., Tsai and Kelly 2005a, b, Tsai 2006, 2007, Ashkezari *et al.* 2008, Mardini and Strauss 2008, Pinarbasi and Mengi 2008, Toopchi-Nezhad *et al.* 2008, Kang and Kang 2009, Toopchi-Nezhad *et al.* 2009).

Experimental and analytical studies (e.g., Gent and Lindley 1959, Tsai 2006) show that compressive behavior of a multilayered rubber bearing can realistically be derived from compressive behavior of its typical interior "bonded" rubber layer. For this reason, in the last century, many researchers have studied bonded rubber layers (refer to Pinarbasi *et al.* (2006, 2008) and Pinarbasi and Mengi (2008) for an extensive list of references). Most of these studies have concentrated on deriving closed-form expressions for compression modulus of rigidly-bonded (simulating steel-reinforced) rubber layers since the vertical stiffness of a rubber bearing directly depends on its compression modulus. Among different analytical approaches used to predict the compression modulus of a bonded rubber layer, the one which is commonly called the "pressure method" is the most widely-used. Originally developed for steel-reinforced rubber bearings (i.e., rigidly-bonded rubber layers), this method considers that the total displacement of a bonded rubber layer is composed of the superposition of two simple displacements; pure homogeneous compression of the corresponding unbonded layer and additional displacement required to keep the points on the bonded surfaces in their original positions (Gent and Lindley 1959). The pressure method is based on three fundamental assumptions: (i) initially vertical lateral surfaces take a parabolic shape in the deformed configuration, (ii) plane sections remain plane and (iii) state of stress at any point in rubber is dominated by the hydrostatic pressure. Advanced analytical studies

in which one/more of the three fundamental assumptions of the pressure method is/are removed (e.g., Papoulia and Kelly 1996, Ling 1996, Tsai and Lee 1998, Pinarbasi *et al.* 2006) have already verified the validity of these assumptions for typical seismic isolation bearings. Thus, the pressure method is now widely used as a handy tool for simplified analysis of typical seismic isolation bearings under compression/bending.

It is worth noting that although the original formulation of the pressure method is based on strict incompressibility assumption, recognizing the significant effect of bulk compressibility of rubber in "thin" rubber layers, this assumption is removed in subsequent formulations. Similarly, even though the original formulation assumes rigid reinforcement, Kelly (1999) showed that the extensibility of the reinforcing sheets can easily be incorporated into the formulation. Kelly and Takhirov (2001, 2002), Tsai and Kelly (2001) and Kelly (2002) have already used the methodology in the analysis of fiber-reinforced rubber bearings.

Even though hollow-circular bearings are also commonly used in many engineering applications, most of the studies in literature have been concentrated on "infinitely" long rectangular bearings or solid circular bearings; only little attention has been given to hollow-circular discs. Studies on annular bearings (e.g., Gent and Lindley 1959, Ling *et al.* 1995, Ling 1996, Pinarbasi *et al.* 2008), all of which have been conducted, to the authors' best knowledge, for steel-reinforced case, have clearly indicated that the presence of even a very small hole in the center of a circular bearing can decrease the compression modulus of the bearing considerably. These studies have also pointed out that the existence of a central hole in a rubber bearing can significantly increase the bonding shear strain under compression as well. It is to be noted that most design codes limit the maximum shear strain developing in a bearing subjected to combined shear and compression, which is computed by adding the shear strain due to shear deformation of the bearing with that due to compression (Kelly 1997). For this reason, besides compression modulus, bonding shear strain is usually accepted as basic design parameters for bridge/seismic isolation bearings. Thus, it is essential that the hole effects on compressive behavior of annular bearing be well understood and properly included in its design.

This paper aims to study, in detail, the compressive behavior of hollow-circular fiber-reinforced rubber bearings (HCFRRBs). The related compression problem is formulated by using the most-recent formulation of the pressure method developed by Kelly (1999), which includes both rubber compressibility and reinforcement flexibility. Particular emphasis is given to the investigation of the effects of reinforcement flexibility and hole presence in view of four key parameters: (i) the stiffness ratio of the reinforcement (relative stiffness of reinforcing sheets with respect to rubber layers), (ii) radius ratio of the hole (ratio of hole radius to outer radius of the bearing), (iii) aspect ratio of the bearing (ratio of outer radius of the bearing to thickness of its individual rubber layers) and (iv) bulk compressibility of rubber.

2. Compression analysis of HCFRRBs by using "modified" pressure method

2.1 Formulation and solution of the problem

Fig. 1(a) illustrates a typical interior "bonded" rubber layer in an HCFRRB. The disc with inner radius *a*, outer radius *R* and uniform thickness *t* is assumed to be perfectly bonded, at its top and bottom faces, to fiber reinforcements made up of many individual fibers, which are modeled as
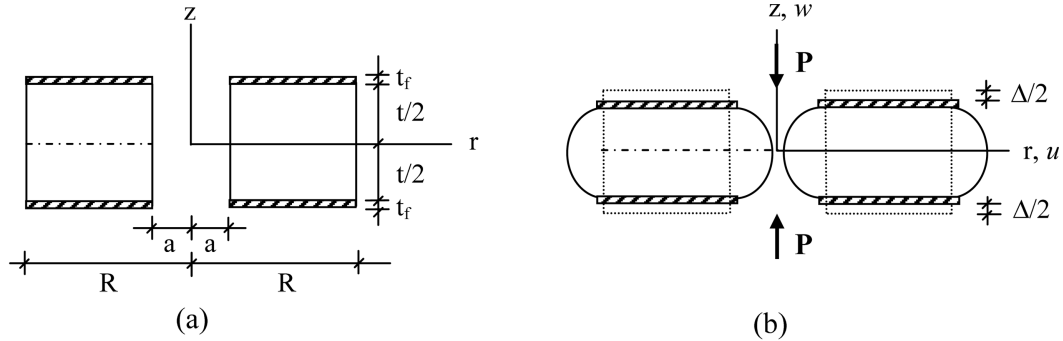
Fig. 1 Uniform compression of an interior "bonded" rubber layer in an HCFRRB

extensible reinforcing sheets of equivalent thickness t_f. When compressed uniformly by a uniaxial force P, the top and bottom reinforcing sheets approach each other with a relative vertical displacement Δ, as illustrated in Fig. 1(b). The object is to formulate this compression problem by using a modified version of the pressure method (Kelly 1999).

A cylindrical coordinate system (r, θ, z) is defined as shown in Fig. 1(a). Since the deformation of the disc is axisymmetric, the displacement component in θ direction vanishes; i.e., $v = 0$, and the displacement components in the other directions are independent of θ; i.e., $u = u(r, z)$, $w = w(r, z)$. The deformed shape of the layer is defined by the kinematic assumptions of the pressure method; i.e., the "parabolic bulging" and "plane sections remain plane" assumptions. As explained in Kelly (1999), the flexibility of the reinforcing sheets can be incorporated into the methodology by supplementing, to the existing parabolic bulging term in radial displacement component, an additional displacement term (u_1) that is constant through the rubber thickness. Thus, the nonzero displacement components can be expressed in the following form

$$u(r,z) = u_0(r)\left(1 - \frac{4z^2}{t^2}\right) + u_1(r) \quad \text{and} \quad w(r,z) = w(z) \tag{1}$$

Although it is common to assume strict incompressibility ($\nu = 0.5$) for rubber, this assumption can lead to overestimated compression stiffness particularly if the "shape factor" of the bearing is large. Shape factor of a multilayered rubber bearing is defined as the ratio of one loaded area to the bulge-free areas for a typical interior rubber layer (Kelly 1997). As an example, for a circular bearing with radius R and thickness of individual rubber layers t, shape factor simply equals to $S = R/2t$. In the case of hollow-circular bearings with inner radius a, outer radius R and thickness of individual rubber layers t, it equals to $S = S_o(1 - \beta)$, where β is the radius ratio for the interior hole and equals to a/R, S_o is called "initial shape factor" (Ling *et al.* 1995) and simply equals to the shape factor of the circular bearing with the same outer radius and interior rubber thickness, i.e., $R/2t$.

To obtain general solutions, the bulk compressibility of rubber is to be included in the present formulation. Thus, the dilatational constitutive relation for the rubber layer can be written as follows

$$\varepsilon_{rr} + \varepsilon_{\theta\theta} + \varepsilon_{zz} = -p/K \tag{2}$$

where ε_{rr}, $\varepsilon_{\theta\theta}$, ε_{zz} are strain components in coordinate directions, K is the bulk modulus of rubber and p is the mean pressure in the rubber. According to the third assumption of the pressure method, the normal stress components in rubber, i.e., σ_{rr}, $\sigma_{\theta\theta}$, σ_{zz}, are all of the same order and their

magnitudes are approximately equal to the mean pressure p.; i.e., $\sigma_{rr} = \sigma_{\theta\theta} = \sigma_{zz} \cong -p$. Axisymmetric strain-displacement relations lead to

$$\varepsilon_{rr} = u_{0,r}\left(1 - \frac{4z^2}{t^2}\right) + u_{1,r}, \quad \varepsilon_{\theta\theta} = \frac{u_0}{r}\left(1 - \frac{4z^2}{t^2}\right) + \frac{u_1}{r}, \quad \varepsilon_{zz} = w_{,z} \quad \text{and} \quad \gamma_{rz} = u_0\left(-\frac{8z}{t^2}\right) \quad (3)$$

where the commas imply partial differentiation with respect to the indicated coordinate and γ_{rz} is the shear strain related to the shear stress component τ_{rz}, which is generated by the constraints at the bonded faces of the rubber layer. Substituting the first three relations in Eq. (3) into Eq. (2) and integrating the resulting equation through the thickness of the rubber layer result in

$$\left[u_{0,r} + \frac{u_0}{r}\right] + \frac{3}{2}\left[u_{1,r} + \frac{u_1}{r}\right] = \frac{3}{2}\frac{\Delta}{t} - \frac{3}{2}\frac{p}{K} \quad (4)$$

When written in terms of the stress components, equilibrium of the rubber layer in radial direction gives

$$\sigma_{rr,r} + \tau_{rz,z} + \frac{\sigma_{rr} - \sigma_{\theta\theta}}{r} = 0 \quad (5)$$

Under the pressure assumption, i.e., with the condition $\sigma_{rr} = \sigma_{\theta\theta} = \sigma_{zz} \cong -p$ and using elastic stress-strain relation for shear behavior of rubber; i.e., $\tau_{rz} = G\gamma_{rz}$, where G is the shear modulus of rubber, with the last relation in Eq. (3), Eq. (5) reduces to
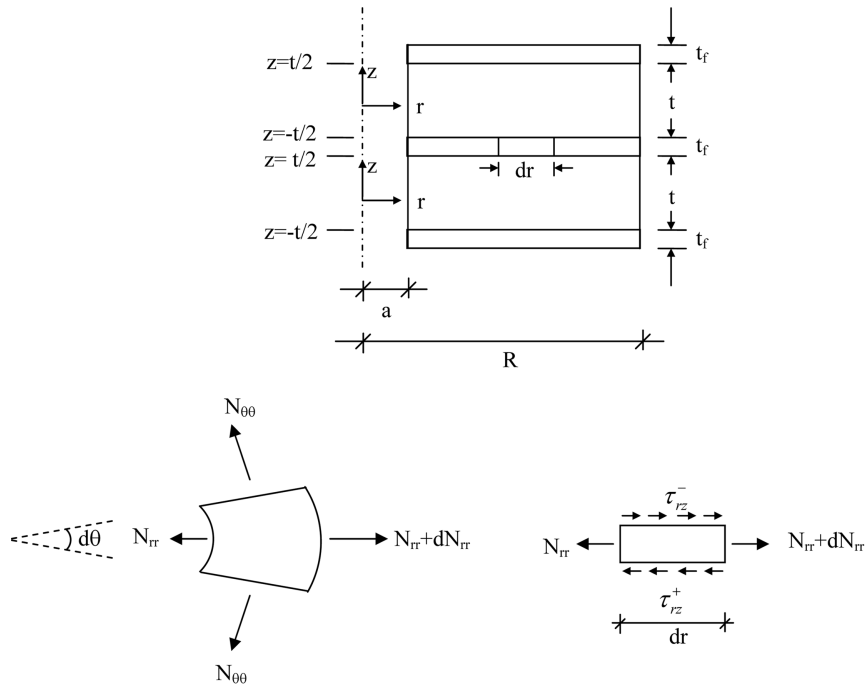
$$p_{,r} = -\frac{8G}{t^2}u_0 \quad (6)$$

Fig. 2 Forces on infinitesimal area of a reinforcing sheet in an HCFRRB (Tsai and Kelly 2001)

Fig. 2 shows the internal forces on infinitesimal area of a reinforcing sheet bonded to rubber layers at its top and bottom surfaces. In the figure, N_{rr} and $N_{\theta\theta}$ denote the stretching forces in the reinforcement per its unit length in radial and circumferential directions respectively while τ_{rz}^- and τ_{rz}^+ denote the bonding shear stresses, i.e., shear stresses applied *from* the rubber layers *to* the reinforcing sheet at its top and bottom faces, which equal to $\tau_{rz}^- = \tau_{rz}(z = -t/2)$ and $\tau_{rz}^+ = \tau_{rz}(z = +t/2)$. It is assumed that the reinforcing sheet is under the influence of plane state of stress. By neglecting the higher order terms, the equilibrium equation for the reinforcing sheet in radial direction can be written as

$$N_{rr,r} + \frac{N_{rr} - N_{\theta\theta}}{r} + \tau_{rz}^- - \tau_{rz}^+ = 0 \tag{7}$$

Using the linear stress-strain relations, internal forces N_{rr} and $N_{\theta\theta}$ can be expressed in terms of u_1 as follows

$$N_{rr} = k_f\left(u_{1,r} + v_f\frac{u_1}{r}\right) \quad \text{and} \quad N_{\theta\theta} = k_f\left(v_f u_{1,r} + \frac{u_1}{r}\right) \quad \text{where} \quad k_f = \frac{E_f t_f}{1 - v_f^2} \tag{8}$$

where k_f is defined as "in-plane stiffness of the reinforcement", E_f and v_f are respectively elasticity modulus and Poisson's ratio of the reinforcing sheet. Substituting Eq. (8) and $\tau_{rz} = -8Gu_0 z/t^2$ into Eq. (7) gives

$$u_{1,rr} + \frac{u_{1,r}}{r} - \frac{u_1}{r^2} = -\frac{8G}{k_f t}u_0 \tag{9}$$

Eqs. (4), (6) and (9) constitute three equations to solve the three unknowns of the problem; u_0, u_1 and p. Taking the derivative of Eq. (4) with respect to r, which gives

$$\left[u_{0,rr} + \frac{u_{0,r}}{r} - \frac{u_0}{r^2}\right] + \frac{3}{2}\left[u_{1,rr} + \frac{u_{1,r}}{r} - \frac{u_1}{r^2}\right] = -\frac{3p_{,r}}{2K} \tag{10}$$

and using Eqs. (6) and (9) in the resulting equation, i.e., in Eq. (10), to eliminate, respectively, the terms in p and u_1, the following second order differential equation for u_0 is obtained

$$u_{0,rr} + \frac{u_{0,r}}{r} - u_0\left[\frac{1}{r^2} + (\beta^*)^2\right] = 0 \quad \text{where} \quad (\beta^*)^2 = \alpha^2 + \lambda^2 \quad \text{with} \quad \alpha^2 = \frac{12G}{k_f t} \quad \text{and} \quad \lambda^2 = \frac{12G}{Kt^2} \tag{11}$$

The solution of Eq. (11) for u_0 is in the following form

$$u_0 = c_1 I_1(\beta^* r) + c_2 K_1(\beta^* r) \tag{12}$$

where c_1 and c_2 are constants to be determined from the boundary conditions of the problem, and, I_1 and K_1 represent, respectively, the modified Bessel functions of first and second kind of order one. Substituting Eq. (12) into Eq. (9), the differential equation for u_1 can also be obtained

$$u_{1,rr} + \frac{u_{1,r}}{r} - \frac{u_1}{r^2} = -\frac{2}{3}\alpha^2[c_1 I_1(\beta^* r) + c_2 K_1(\beta^* r)] \tag{13}$$

which has the solution in the following form

$$u_1 = -\frac{2}{3}\frac{\alpha^2}{(\beta^*)^2}[c_1 I_1(\beta^* r) + c_2 K_1(\beta^* r)] + c_3\frac{r}{2} + c_4\frac{1}{r} \tag{14}$$

where c_3 and c_4 are additional integration constants. Stress-free boundary conditions at the bulge-free faces of the rubber layer; i.e., $p(a;R) = 0$, and force-free boundary conditions at the edges of the reinforcing sheet; i.e., $N_{rr}(a;R) = 0$, provide four conditions to solve four unknown integration constants. Since the boundary conditions are defined in terms of p and N_{rr}, it is convenient to write them in terms of the integration constants by substituting Eqs. (12) and (14) respectively into Eq. (4) and into the first of Eq. (8)

$$p = K\frac{\Delta}{t} - \frac{2K\lambda^2}{3\ \beta^*}[c_1 I_0(\beta^* r) - c_2 K_0(\beta^* r)] - c_3 K \tag{15}$$

$$N_{rr} = k_f\left[-\frac{2\alpha^2}{3\beta^*}\left\{[c_1 I_0(\beta^* r) - c_2 K_0(\beta^* r)] - (1 - v_f)\left[\frac{c_1 I_1(\beta^* r) + c_2 K_1(\beta^* r)}{(\beta^* r)}\right]\right\} + \frac{(1 + v_f)}{2}c_3 - (1 - v_f)\frac{c_4}{r^2}\right] \tag{16}$$

where I_0 and K_0 represent, respectively, the modified Bessel functions of first and second kind of order zero. Stress boundary conditions for the rubber layer; i.e., $p(a) = 0$ and $p(R) = 0$, imply

$$K\frac{\Delta}{t} - \frac{2K\lambda^2}{3\ \beta^*}[c_1 I_0(\beta^* R) - c_2 K_0(\beta^* R)] = c_3 K \text{ and } K\frac{\Delta}{t} - \frac{2K\lambda^2}{3\ \beta^*}[c_1 I_0(\beta^* a) - c_2 K_0(\beta^* a)] = c_3 K \tag{17}$$

By eliminating c_3 from Eq. (17), c_2 can be written in terms of c_1 as

$$c_2 = A_1 c_1 \text{ where } A_1 = \frac{I_0(\beta^* R) - I_0(\beta^* a)}{K_0(\beta^* R) - K_0(\beta^* a)} \tag{18}$$

Then, substituting Eq. (18) into the first of Eq. (17), c_3 can be obtained in terms of c_1 as

$$c_3 = \frac{\Delta}{t} - \frac{2}{3}\frac{\lambda^2}{\beta^*}c_1[I_0(\beta^* R) - A_1 K_0(\beta^* R)] \tag{19}$$

Using Eq. (18), the reinforcement-related boundary conditions can be written in the following simpler form

$$\left[-\frac{2}{3}\frac{\alpha^2}{\beta^*}c_1 A_2 + \frac{(1 + v_f)}{2}c_3 - (1 - v_f)\frac{c_4}{R^2}\right] = 0 \text{ and } \left[-\frac{2}{3}\frac{\alpha^2}{\beta^*}c_1 A_3 + \frac{(1 + v_f)}{2}c_3 - (1 - v_f)\frac{c_4}{a^2}\right] = 0 \tag{20}$$

where

$$A_2 = [I_0(\beta^* R) - A_1 K_0(\beta^* R)] - (1 - v_f)\left[\frac{I_1(\beta^* R) + A_1 K_1(\beta^* R)}{(\beta^* R)}\right]$$

$$A_3 = [I_0(\beta^* a) - A_1 K_0(\beta^* a)] - (1 - v_f)\left[\frac{I_1(\beta^* a) + A_1 K_1(\beta^* a)}{(\beta^* a)}\right] \tag{21}$$

Finally, by eliminating c_4 from Eq. (20) and using Eq. (19), c_1 is obtained as follows

$$c_1 = \frac{3\Delta}{2}\frac{\beta^*}{t}\frac{(1 + v_f)}{\alpha^2}\left(1 - \frac{a^2}{R^2}\right)\frac{1}{A_2 - \frac{a^2}{R^2}A_3 + \left(1 - \frac{a^2}{R^2}\right)A_4} \tag{22}$$

where

$$A_4 = \frac{(1+\nu_f)}{2}\frac{\lambda^2}{\alpha^2}[I_0(\beta^*R)-A_1K_0(\beta^*R)] \tag{23}$$

Finally, by eliminating c_3 from Eq. (20), one can write c_4 in terms of c_1 as follows

$$c_4 = \frac{2}{3}\frac{\alpha^2}{\beta^*}c_1\frac{a^2}{\left(1-\dfrac{a^2}{R^2}\right)}\frac{(A_2-A_3)}{(1-\nu_f)} \tag{24}$$

The vertical stiffness K_v of a multilayered rubber bearing is defined as (Naeim and Kelly 1999)

$$K_v = \frac{E_cA}{t_r} \tag{25}$$

where A is the area of the reinforcing sheets, t_r is the total rubber thickness in the bearing and E_c is named as effective compression modulus, or simply "compression modulus". Compression modulus of a rubber bearing is controlled by its "bonded" rubber layers and is determined from the ratio of nominal compressive stress σ_c to nominal compression strain ε_c

$$E_c = \frac{\sigma_c}{\varepsilon_c} = \frac{P/A}{\Delta/t} \tag{26}$$

The total compressive force P can be determined by integrating the pressure over the bonded area. Noting that $K\dfrac{\lambda^2}{\alpha^2} = \dfrac{k_f}{t}$, pressure distribution in the rubber layer can be written as

$$p = \frac{k_f}{t}\frac{\Delta}{t}\frac{(1+\nu_f)}{2}\left(1-\frac{a^2}{R^2}\right)\frac{[I_0(\beta^*R)-I_0(\beta^*r)]-A_1[K_0(\beta^*R)-K_0(\beta^*r)]}{A_2-\dfrac{a^2}{R^2}A_3+\left(1-\dfrac{a^2}{R^2}\right)A_4} \tag{27}$$

which, when integrated over the bonded area and divided to $A\varepsilon_c$, where $A = \pi(R^2-a^2)$, gives the following closed-form expression for compression modulus of hollow-circular fiber-reinforced bearings, which will be denoted in this paper as $E_{c,HC}$

$$E_{c,HC} = \frac{k_f}{t}\frac{(1+\nu_f)}{2}\frac{\left\{ \begin{array}{c} \left(1-\dfrac{a^2}{R^2}\right)[I_0(\beta^*R)-A_1K_0(\beta^*R)] \\ -2\left[\dfrac{I_1(\beta^*R)+A_1K_1(\beta^*R)}{(\beta^*R)}\right]+\dfrac{2a^2}{R^2}\left[\dfrac{I_1(\beta^*a)+A_1K_1(\beta^*a)}{(\beta^*a)}\right] \end{array} \right\}}{A_2-\dfrac{a^2}{R^2}A_3+\left(1-\dfrac{a^2}{R^2}\right)A_4} \tag{28}$$

Since another concern in the design of annular bearings is the maximum (absolute) shear strain generated in the rubber layer by compression, denoted in this paper as, $\gamma_{max,HC}$, which occurs at the bonded faces of rubber layers (i.e., when $z = \pm t/2$), its closed-form expression also deserves presenting here

$$\gamma_{\max,HC} = \frac{6\beta^*}{\alpha^2 t}\frac{\Delta(1+v_f)}{t}\left(1-\frac{a^2}{R^2}\right)\frac{[I_1(\beta^* r)+A_1 K_1(\beta^* r)]}{A_2 - \frac{a^2}{R^2}A_3 + \left(1-\frac{a^2}{R^2}\right)A_4}$$
(29)

2.2 Convergence of the solution to some special limiting cases

The results obtained in the previous section are general in the sense that they include the effects of three basic parameters: (i) the presence of a central circular hole in the bearing, (ii) compressibility of the rubber layer and (iii) extensibility of the reinforcing sheets. There are various special cases which can be used to verify the accuracy of these results, such as the cases which neglect the effects of the rubber compressibility and/or reinforcement extensibility and/or hole existence.

Each case can be analyzed separately. If the effect of rubber compressibility is desired to be neglected, the dilatational constitutive equation used in the above formulation has to be changed with the incompressibility condition (i.e., $\varepsilon_{rr}+\varepsilon_{\theta\theta}+\varepsilon_{zz}=0$). Or if, instead of an annular circular bearing, a solid circular bearing is desired to be analyzed, the boundary conditions written on the hole (i.e., at $r=a$) has to be replaced with the conditions that stresses in the rubber layer and forces in the reinforcement have to be finite at the center of the bearing (i.e., at $r=0$). Else, if, instead of a fiber-reinforced bearing, a steel-reinforced bearing is desired to be analyzed, the term representing the reinforcement extensibility in radial displacement component has to be removed from the formulation (i.e., $u_1=0$). To have consistent and comparable results, each of these extreme cases, some of which are also available in literature in different forms, has been analyzed separately (not presented here). The closed-form expressions derived for each case are used to check the convergence of the general expressions derived in this study.

2.2.1 Hollow-circular fiber-reinforced bearings, effect of compressibility neglected

The first limiting case that deserves discussing in this paper is the incompressible case, which, similar to the compressible case, has not been published in literature, yet (to the best knowledge of authors). Although the inclusion of rubber compressibility is essential for accurate prediction of E_c of high shape factor bearings, incompressibility assumption can realistically be used in low shape factor bearings. E_c of a hollow-circular fiber-reinforced rubber bearing with the assumption of incompressibility, denoted in this paper as $E_{c,HC,incomp}$, can be obtained from Eq. (28) by letting $K \to \infty$, which means $\lambda \to 0$, or, $\beta^* = \alpha$

$$E_{c,HC,incomp} = \frac{k_f(1+v_f)}{t}\frac{}{2}\frac{\left\{\begin{array}{c}\left(1-\frac{a^2}{R^2}\right)[I_0(\alpha R)-A_1 K_0(\alpha R)] \\ -2\left[\dfrac{I_1(\alpha R)+A_1 K_1(\alpha R)}{(\alpha R)}\right]+\dfrac{2a^2}{R^2}\left[\dfrac{I_1(\alpha a)+A_1 K_1(\alpha a)}{(\alpha a)}\right]\end{array}\right\}}{A_2 - \frac{a^2}{R^2}A_3}$$
(30)

2.2.2 Hollow-circular steel-reinforced bearings, effect of compressibility included

In case of a steel-reinforced bearing, the extensibility of rigid steel plates is neglected, which can

be reflected to Eq. (28) by allowing $k_f \to \infty$, implying $\alpha \to 0$, thus, $\beta^* = \lambda$. Before applying the limits, by recalling that $k_f/t = K\lambda^2/\alpha^2$, it is convenient to rewrite Eq. (28) as

$$
E_{c,HC} = K\frac{(1+v_f)}{2}\frac{\dfrac{\lambda^2}{\alpha^2}\left\{\begin{array}{c}\left(1-\dfrac{a^2}{R^2}\right)[I_0(\beta^*R)-A_1K_0(\beta^*R)]\\[2mm]-2\left[\dfrac{I_1(\beta^*R)+A_1K_1(\beta^*R)}{(\beta^*R)}\right]+\dfrac{2a^2}{R^2}\left[\dfrac{I_1(\beta^*a)+A_1K_1(\beta^*a)}{(\beta^*a)}\right]\end{array}\right\}}{A_2-\dfrac{a^2}{R^2}A_3+\left(1-\dfrac{a^2}{R^2}\right)\dfrac{(1+v_f)}{2}\dfrac{\lambda^2}{\alpha^2}[I_0(\beta^*R)-A_1K_0(\beta^*R)]}
\tag{31}
$$

Then, in the limiting case, when $\alpha \to 0$, $\beta^* = \lambda$, and $\lambda^2/\alpha^2 \to \infty$, E_c of hollow-circular steel-reinforced bearings which includes the effect of bulk compressibility, denoted in this paper as $E_{c,HC,SR}$, is obtained as

$$
E_{c,HC,SR} = K\frac{\left(1-\dfrac{a^2}{R^2}\right)[I_0(\lambda R)-A_1K_0(\lambda R)]-2\left[\dfrac{I_1(\lambda R)+A_1K_1(\lambda R)}{(\lambda R)}\right]+\dfrac{2a^2}{R^2}\left[\dfrac{I_1(\lambda a)+A_1K_1(\lambda a)}{(\lambda a)}\right]}{\left(1-\dfrac{a^2}{R^2}\right)[I_0(\lambda R)-A_1K_0(\lambda R)]}
\tag{32}
$$

where

$$
A_1 = \frac{I_0(\lambda R)-I_0(\lambda a)}{K_0(\lambda R)-K_0(\lambda a)}
\tag{33}
$$

Eq. (32) can further be reduced to

$$
E_{c,HC,SR} = K\left\{1-\frac{2}{\left(1-\dfrac{a^2}{R^2}\right)}\frac{\left(\dfrac{I_1(\lambda R)+A_1K_1(\lambda R)}{(\lambda R)}\right)-\dfrac{a^2}{R^2}\left(\dfrac{I_1(\lambda a)+A_1K_1(\lambda a)}{(\lambda a)}\right)}{I_0(\lambda R)-A_1K_0(\lambda R)}\right\}
\tag{34}
$$

2.2.3 Circular fiber-reinforced bearings, effect of compressibility included

E_c of a circular fiber-reinforced bearing which includes the effect of rubber compressibility, denoted in this paper as $E_{c,C}$, can be obtained from Eq. (28) by removing the effects of the hole at the center of the bearing, i.e., by letting $a/R \to 0$. For such a case, the terms containing modified Bessel functions of second kind (i.e., K_0 and K_1) drop. Thus, $E_{c,C}$ becomes

$$
E_{c,C} = \frac{k_f}{t}\frac{(1+v_f)}{2}\frac{\left\{[I_0(\beta^*R)]-2\left[\dfrac{I_1(\beta^*R)}{(\beta^*R)}\right]\right\}}{A_2+A_4}
\tag{35}
$$

where

$$A_2 = I_0(\beta^* R) - (1 - v_f)\frac{I_1(\beta^* R)}{(\beta^* R)} \text{ and } A_4 = \frac{(1 + v_f)}{2}\frac{\lambda^2}{\alpha^2}I_0(\beta^* R) \tag{36}$$

Eq. (35) can be written in a more compact form as follows

$$E_{c,C} = \frac{k_f(1 + v_f)}{t}\frac{I_0(\beta^* R) - \frac{2I_1(\beta^* R)}{(\beta^* R)}}{\left[1 + \frac{(1 + v_f)}{2}\frac{\lambda^2}{\alpha^2}\right]I_0(\beta^* R) - (1 - v_f)\frac{I_1(\beta^* R)}{(\beta^* R)}} \tag{37}$$

2.2.4 Circular fiber-reinforced bearings, effect of compressibility neglected

E_c of a circular fiber-reinforced bearing which neglects the effect of rubber compressibility, denoted as $E_{c,C,incomp}$, can be obtained by simplifying Eq. (35) further using $K \to \infty$, which implies $\lambda \to 0$, i.e., $\beta^* = \alpha$. Thus, similar to the hollow-circular case studied in Section 2.2.1, it is sufficient to remove A_4 term and replace all α's with β^*'s, which results in

$$E_{c,C,incomp} = \frac{k_f(1 + v_f)}{t}\frac{I_0(\alpha R) - \frac{2I_1(\alpha R)}{(\alpha R)}}{I_0(\alpha R) - (1 - v_f)\frac{I_1(\alpha R)}{(\alpha R)}} \tag{38}$$

It can easily be shown that Eq. (38) is the same as the expression given in Tsai and Kelly (2001).

2.2.5 Circular steel-reinforced bearings, effect of compressibility included

Recalling that $k_f/t = K\lambda^2/\alpha^2$, Eq. (37) can be rewritten in the following form

$$E_{c,C} = K\frac{\frac{\lambda^2}{\alpha^2}\frac{(1 + v_f)}{2}\left[I_0(\beta^* R) - \frac{2I_1(\beta^* R)}{(\beta^* R)}\right]}{\frac{\lambda^2}{\alpha^2}\frac{(1 + v_f)}{2}[I_0(\beta^* R)] + \left[I_0(\beta^* R) - (1 - v_f)\frac{I_1(\beta^* R)}{(\beta^* R)}\right]} \tag{39}$$

When $k_f \to \infty$, $\alpha \to 0$ and $\beta^* = \lambda$. Thus, in the limiting case when $\lambda^2/\alpha^2 \to \infty$, Eq. (39) reduces to the following simple expression for E_c of a circular steel-reinforced bearing which includes the effect of bulk compressibility, denoted in this paper as $E_{c,C,SR}$

$$E_{c,C,SR} = K\left[1 - \frac{2I_1(\lambda R)}{I_0(\lambda R)(\lambda R)}\right] \tag{40}$$

which is identical to the expression presented in Kelly (1997). As shown by Kelly (1997), this expression satisfactorily reduces to the following well-known expression derived for circular steel-reinforced bearings with the assumption of incompressibility, denoted as $E_{c,C,SR,incomp}$

$$E_{c,C,SR,incomp} = 6GS^2 \quad \text{and} \quad S = \frac{R}{2t} \tag{41}$$

At this point, it is to be noted that the formulation used in this study does *not* include the first stage solutions; i.e., the solutions coming from the homogenous compression of the rubber layer. In other

words, the above-presented E_c expressions only include the second stage solutions. Since the shape-factor-dependent expressions obtained from second stage solutions are usually much larger than the shape-factor-independent expressions coming from first stage solutions (unless the shape factor of the bearing is considerably low), such a simplification is possible for practical seismic isolation bearings (Kelly 1997). In case of bearings with small shape factors, it is strongly recommended that the constant-term coming from the first-stage solutions, which is simply equal to the modulus of elasticity (E) of rubber in case of an annular bearing, be added to the E_c expressions presented above.

3. Discussions

From Eq. (27) to Eq. (29), it may be noticed that the compressive behavior of a HCFRRB is controlled by four main parameters: (i) the extensibility of fiber-reinforcement, (ii) size of the centrally-placed hole, (iii) aspect ratio of the interior "reinforced" rubber layers and (iv) bulk compressibility of the rubber. In this section of the paper, the effects of each factor on two basic design parameters; namely, compression modulus and maximum bonding shear strain, are investigated thoroughly.

For easier presentations and discussions, some nondimensionalized parameters are defined. Denoted as k_f^*, which equals to k_f/Gt, the "stiffness ratio" of the bearing provides a measure on relative "stiffness" of the reinforcing sheets compared to the rubber layers. Since as shown by Tsai and Kelly (2001), the individual effect of v_f on compressive behavior of the bearings is *not* major, v_f is *not* considered as a variable of the parametric study, instead, it is fixed to a common value of $v_f = 0.3$, as done in Tsai and Kelly (2001). The second parameter, "radius ratio", denoted as β, provides a measure on relative size of the hole and is simply defined as $\beta = a/R$. Incorporation of the third parameter; i.e., aspect ratio of interior "bonded" rubber layers, into the numerical study of annular rubber bearings, however, is not as straightforward as in circular bearings. Unlike a circular bearing, for which the shape factor (the ratio of one bonded area to its bulge free area) is $S = R/2t$, it is *not* possible to relate the shape factor of an annular bearing, which is $S = S_o(1-\beta)$ where $S_o = R/2t$, *directly* to the aspect ratio of the interior rubber layers. It can be noticed that S_o, called "initial shape factor" (Ling *et al.* 1995), simply equals to the shape factor of the circular bearing with the same outer radius and interior rubber thickness. Considering that β has already been selected as one of the basic parameters governing the compressive behavior of annular bearings, instead of S, S_o is selected as the third parameter of the study. Finally, as emphasized by the earlier studies, since ignoring the bulk compressibility of rubber can lead to overestimation of compression modulus for bearings with high shape factors, rubber compressibility is included in the numerical study as the fourth parameter. Plotting the graphs in terms of either Poisson's ratio v or "relative" bulk compressibility K/G of rubber is possible. Recalling the relation between these two material constants, i.e., $K/G = [2(1+v)]/[3(1-2v)]$, the conversion between them can easily be made whenever required. It is also to be noted that since the basic assumptions of the pressure method may *not* be valid for highly compressible materials, the lower limit of v is selected in the numerical analysis as $v = 0.49$, which corresponds to highly compressible rubber with $K = 50G$.

3.1 Compression modulus

Fig. 3 shows the variation of compression modulus of HCFRRBs ($E_{c,HC}$) with stiffness ratio ($k_f^* = k_f/Gt$) for two specific values of initial shape factors; $S_o = 5$, representing low shape factor (LSF)
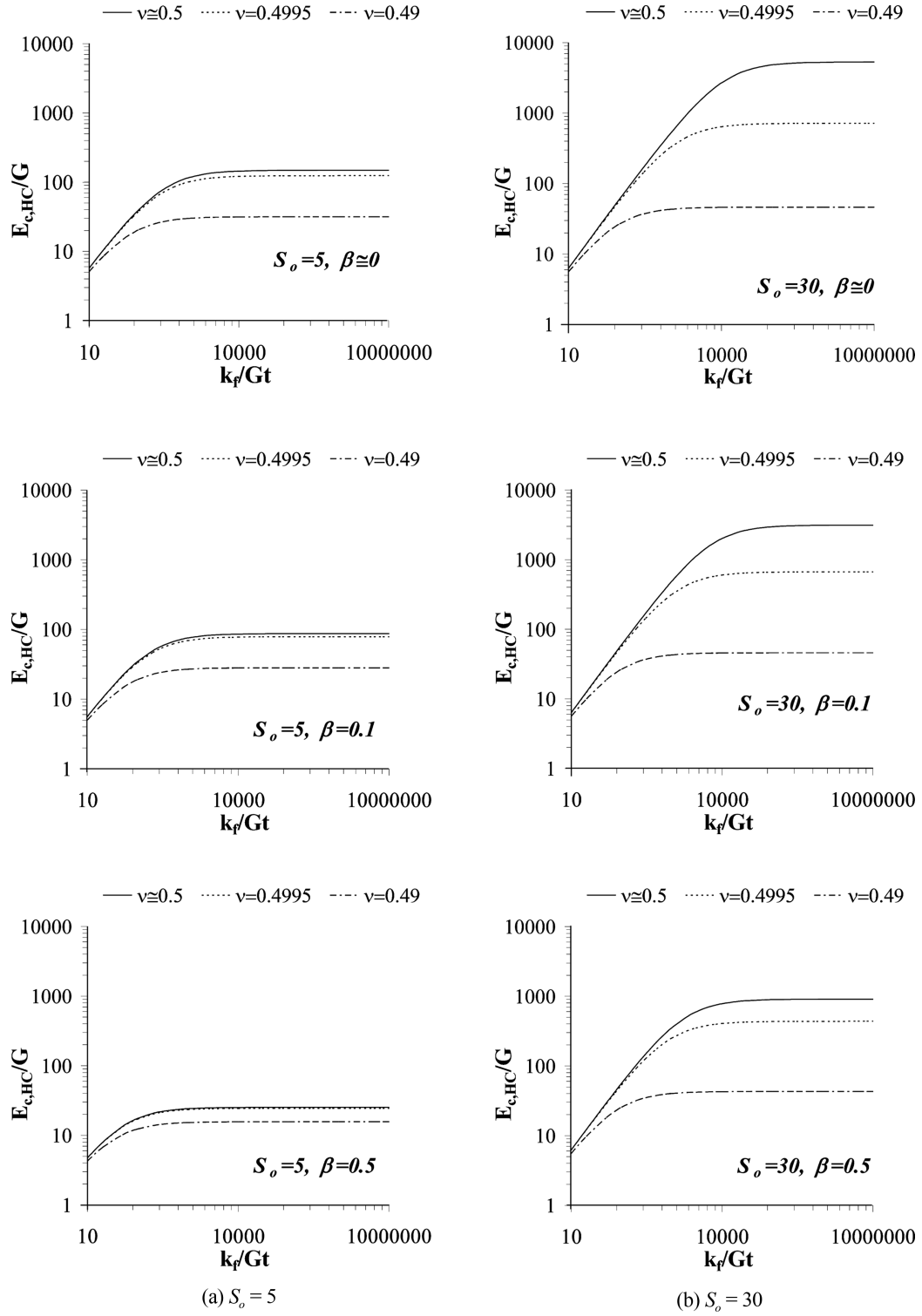
(a) $S_o = 5$ (b) $S_o = 30$

Fig. 3 Effect of reinforcement flexibility on compression modulus

bearings and $S_0 = 30$, representing high shape factor (HSF) bearings. The effect of rubber compressibility is also studied in the graphs, which are plotted for three different values of Poisson's ratio; $\nu = 0.49$, corresponding to highly compressible rubber with $K = 50G$, $\nu = 0.4995$, corresponding to natural rubber with $K = 1000G$, and $\nu = 0.4999999$, which is considered to be sufficiently close to the incompressible value of 0.5, corresponding to $K/G \to \infty$. Also, the graphs are plotted for three different values of radius ratio; $\beta \cong 0$, implying a solid section, $\beta = 0.1$, representing a medium-sized hole, and $\beta = 0.5$, representing a considerably large hole. Noticing that the graphs presented in Fig. 3 are plotted in log-log scale and comparing the graphs in Fig. 3(a) with those in Fig. 3(b), one can see the great effect of shape factor on compression modulus. As expected, the compression modulus of a fiber-reinforced bearing asymptotically approaches to the compression modulus of its "equivalent" (i.e., with identical S_o, β and ν) steel-reinforced bearing as k_f^* increases. While an HSF bearing reaches its asymptotic value at considerably large values of k_f^*, particularly if rubber compressibility is very low, there is no need to have very large values of k_f^* for an LSF bearing to behave as if it were steel-reinforced. Such a behavior can also be observed from the comparison of the graphs plotted for bearings with identical S_o and ν but different β values; as β increases, the limiting k_f^* value decreases. While the curves plotted in Fig. 3(a) for the bearing with $S_o = 5$ composed of nearly ($\nu = 0.4995$) and strictly ($\nu \cong 0.5$) incompressible rubber almost coincide, showing that slight compressibility of rubber can realistically be ignored in the design of LSF bearings, those in Fig. 3(b) for the bearing with $S_o = 30$ deviate from each other considerably, indicating the significant effect of compressibility in HSF bearings. One can also observe from Fig. 3 that for the bearing with the same S_o and β, as ν decreases, the limiting k_f^* value at which the steel-reinforced bearing behavior is attained decreases.

Since $E_{c,HC}$ of an LSF bearing can be much smaller than $E_{c,HC}$ of an HSF bearing for an easier and more accurate evaluation of the effects of k_f^* on bearings with different S_o values, it can be helpful to replot the graphs in Fig. 3 by normalizing the modulus values with respect to their limiting values computed for the corresponding (i.e., with identical S_o, β and ν) steel-reinforced bearings ($E_{c,HC,SR}$). Such graphs are presented in Fig. 4. Since the behavior change from LSF bearings to HSF bearings is very rapid, the graphs plotted for bearings with an intermediate initial shape factor, $S_o = 15$, representing moderate shape factor (MSF) bearings, are also included in these normalized graphs. As it is apparent from Fig. 4(b), the curves plotted for MSF bearings, thus their compressive behavior, lay in between those for LSF and HSF bearings.

The effects of β on $E_{c,HC}$ are more apparent in the graphs presented in Fig. 5, which are plotted for $S_o = 5$, 15 and 30, and for two specific values of stiffness ratio: $k_f^* = 30000$ and $k_f^* = 300$, corresponding respectively to a relatively stiff and highly extensible reinforcing sheets. In the graphs, modulus values are normalized with respect to their limiting values computed for the corresponding (i.e., with identical S_o, k_f^* and ν) circular bearings ($E_{c,C}$) so that the decrease in compression modulus due to the hole existence can directly be seen. Investigation of the behavior of the bearings when $k_f^* = 30000$ is valuable in view of that this particular value of k_f^* is calculated using $E_f = 210$ GPa, $\nu_f = 0.3$, $t_f = 0.27$ mm, $t = 3$ mm, $G = 0.7$ MPa, which represent the geometric and material properties of fiber-reinforced seismic isolation bearings tested by Kelly (2002). In fact, as it is apparent from Fig. 4, the value of 30000 is a sufficiently large value for k_f^*, even for the HSF bearing ($S_o = 30$), to use $E_{c,HC,SR}$ instead of $E_{c,HC}$ in the design of fiber-reinforced bearings provided that $\nu \leq 0.4995$. Fig. 5(a) show how fast $E_{c,HC}$ decreases with increasing β if $\nu = 0.5$ and $k_f^* = 30000$. The presence of slight compressibility ($\nu = 0.4995$) reduces this effect considerably in HSF and MSF bearings. From the comparison of Fig. 5(a) with Fig. 5(b), it is seen that if k_f^*
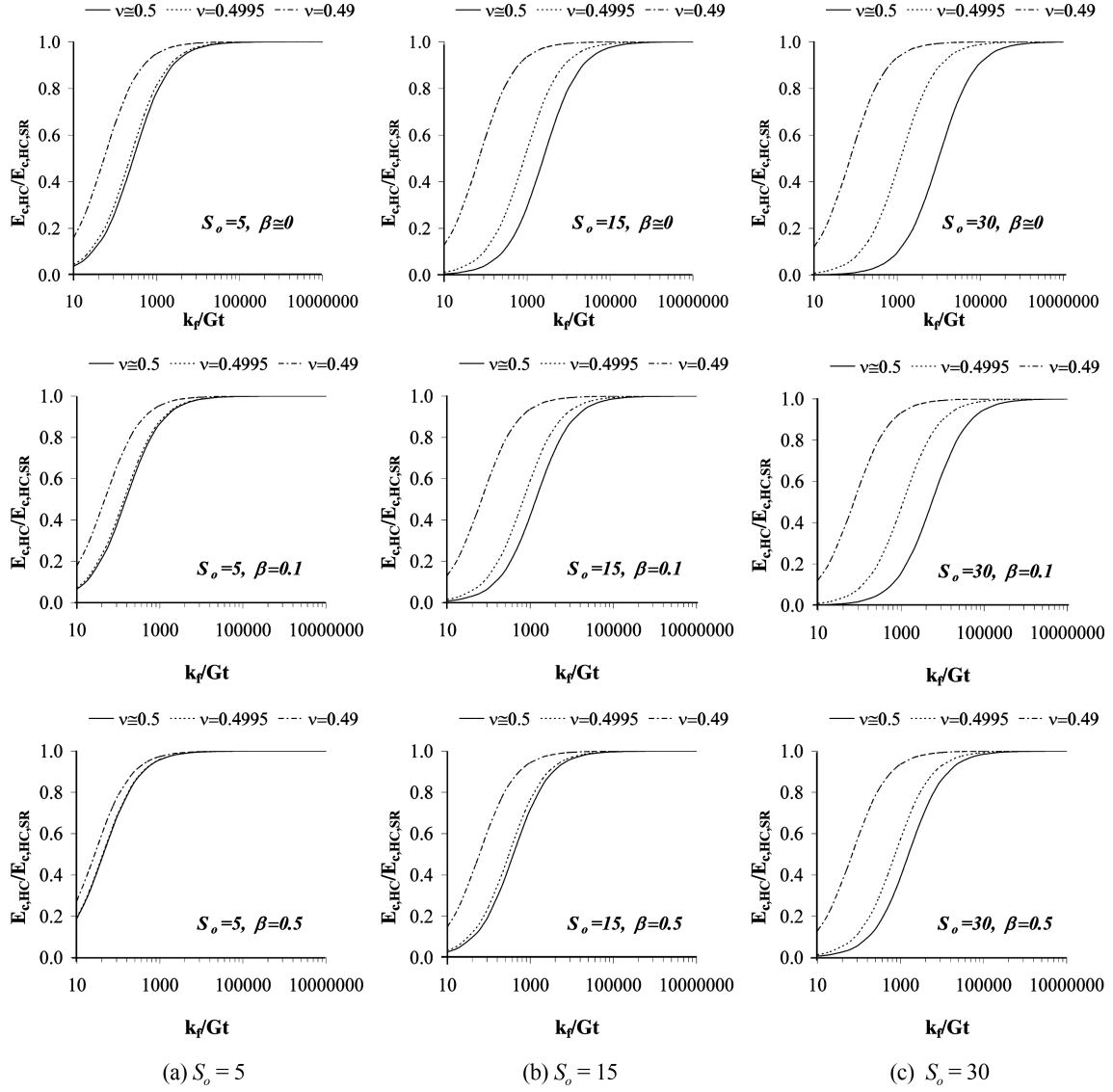
Fig. 4 Effect of reinforcement flexibility on normalized compression

decreases, the bearings, particularly the MSF and HSF bearings, become less sensitive to the hole effects unless β is considerably large.

The effects of rubber compressibility on $E_{c,HC}$ are more apparent from Fig. 6, which shows its variation with v or K/G for various geometric and material properties. In the graphs, modulus values are normalized with respect to those computed ignoring bulk compressibility of rubber ($E_{c,HC,incomp}$) so that the decrease in compression modulus due to rubber compressibility can directly be seen. The S-shaped curves show how incompressible behavior is approached as v increases. The earlier conclusion that the bearings with smaller S_o and/or k_f^* reach their incompressible values at much smaller values of v is now more apparent. These graphs also show why $E_{c,HC}$ of an HSF bearing
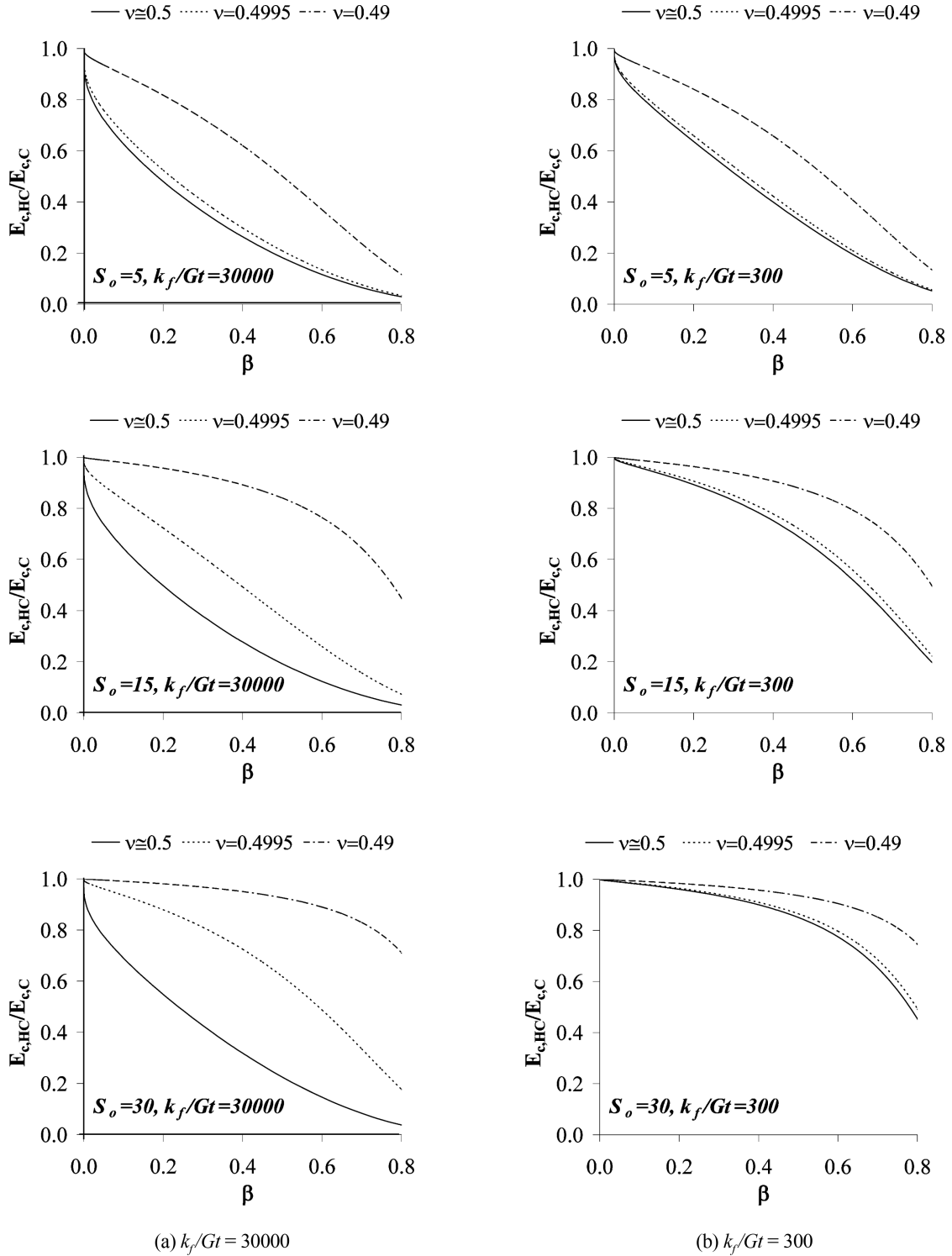
(a) $k_f/Gt = 30000$ (b) $k_f/Gt = 300$

Fig. 5 Effect of radius ratio on normalized compression modulus

with $k_f^* = 30000$ decrease significantly when $\nu = 0.4995$ while an LSF bearing does not "sense" such small compressibility.
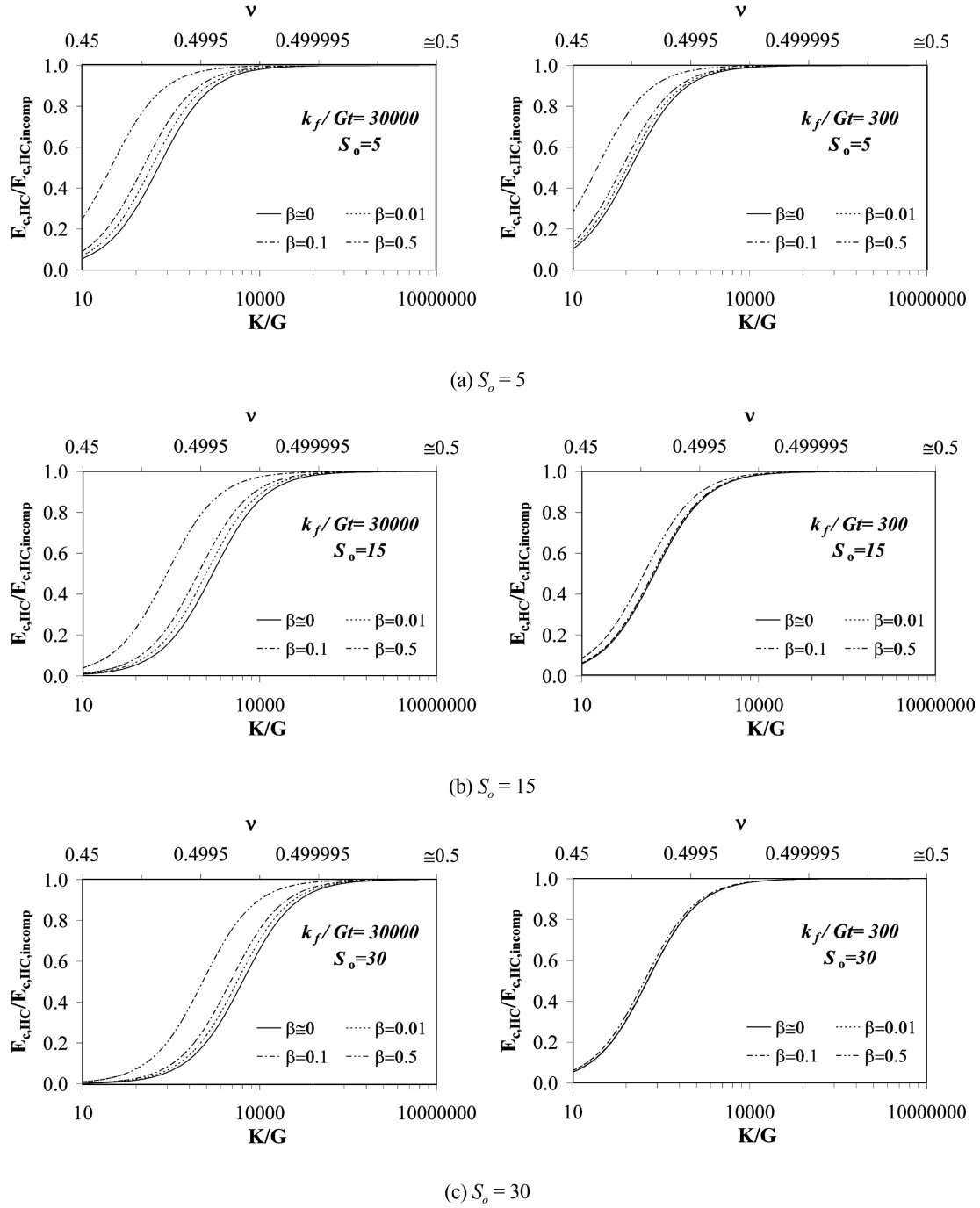

(a) $S_o = 5$

(b) $S_o = 15$

(c) $S_o = 30$

Fig. 6 Effect of rubber compressibility on normalized compression modulus

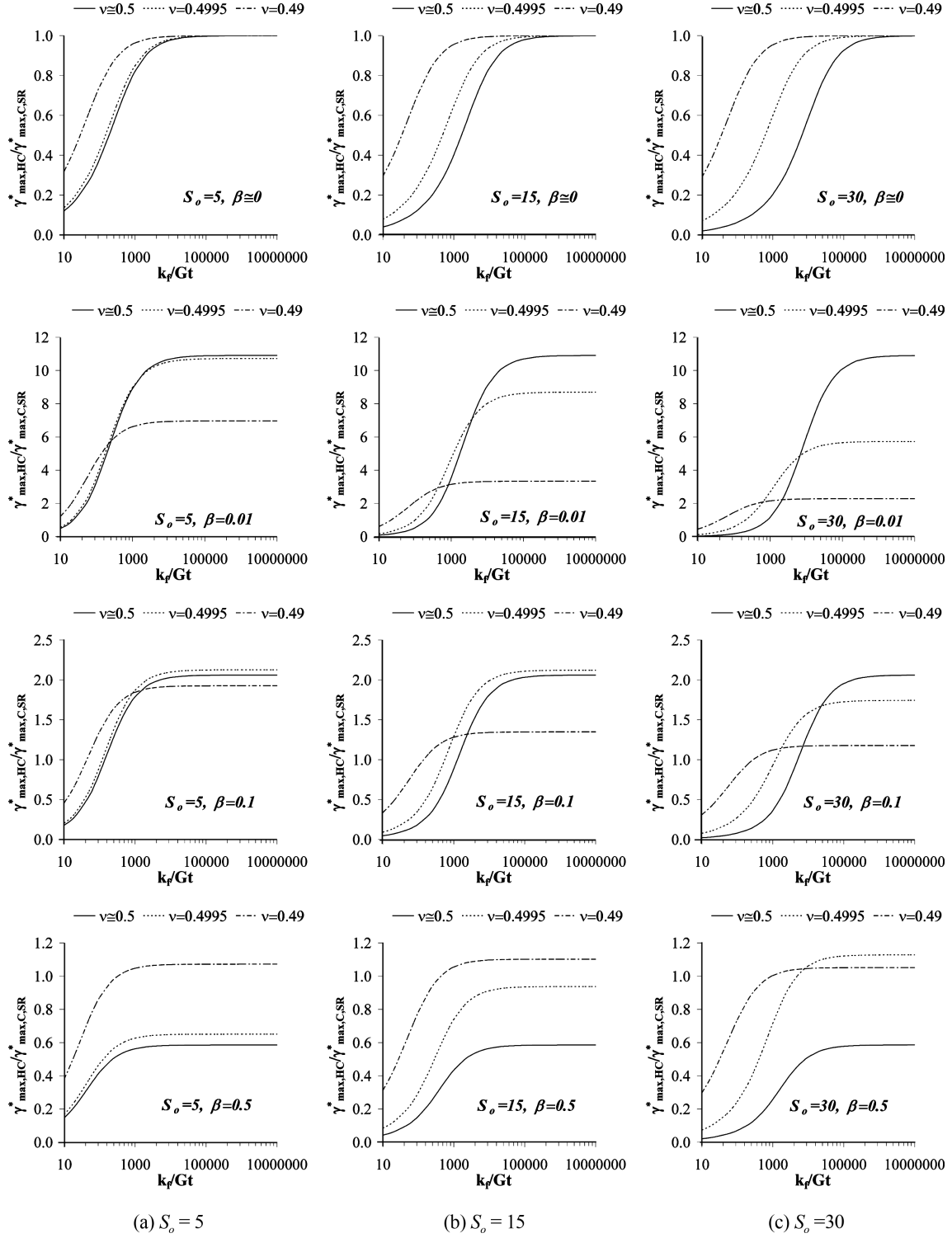(a) $S_o = 5$ (b) $S_o = 15$ (c) $S_o = 30$

Fig. 7 Variation of "magnification factor" with reinforcement flexibility

3.2 Maximum shear strain

A detailed study on shear stress distributions in an HCFRRB shows that one of the major effects of the existence of a hole in a fiber-reinforced bearing is the increase in shear stress, thus, shear strain, developing in the bearing under compression. Considering that maximum shear strain generated in the bearing by compression has to be added to that by shear to compute the maximum total shear strain developing in a compression-shear bearing and noting that this maximum value of the shear strain is usually limited to some code-defined values in the design of the bearing, it is important to investigate how it is affected from the reinforcement flexibility in HCFRRBs. The graphs shown in Fig. 7 illustrate this effect for various geometric and material properties. In Fig. 7, γ_{max}^{*} denotes the ratio of maximum shear strain developing in the bearing due to compression to the applied compression strain; i.e., $\gamma_{max}^{*} = \gamma_{max} / \varepsilon_c$. γ_{max}^{*} values of HCFRRBs ($\gamma_{max,HC}^{*}$) are normalized with respect to γ_{max}^{*} values of corresponding (i.e., with identical S_o, k_f^{*} and v) circular steel-reinforced rubber bearings ($\gamma_{max,C,SR}^{*}$), which is defined in this paper as "magnification factor (f)". It

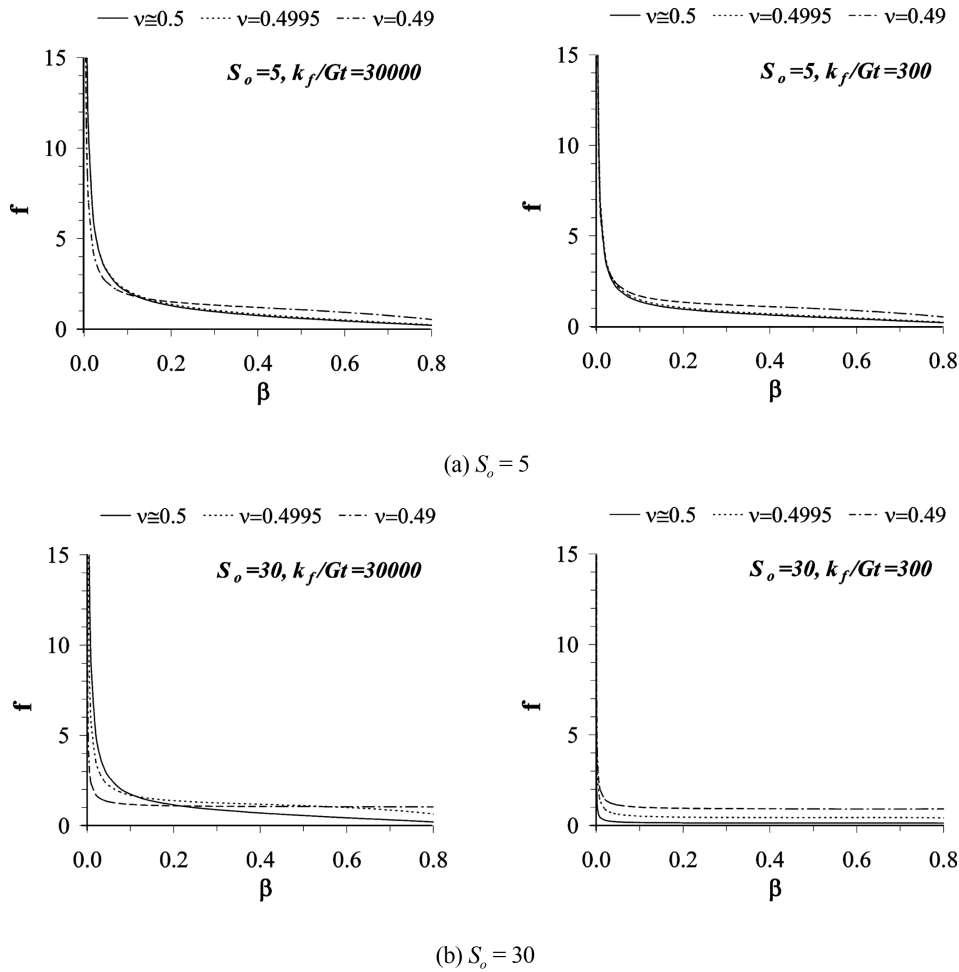(a) $S_o = 5$

(b) $S_o = 30$

Fig. 8 Variation of "magnification factor" with radius ratio

is worth noting that $\gamma^*_{max,C,SR} = 6S_o$ when $v = 0.5$. As expected, f decreases as k^*_f decreases. The effect of k^*_f on f is similar to its effect on E_c. S-shaped curves define the limiting k^*_f values above which a fiber-reinforced bearing behaves as if steel-reinforced. f values computed for a very small
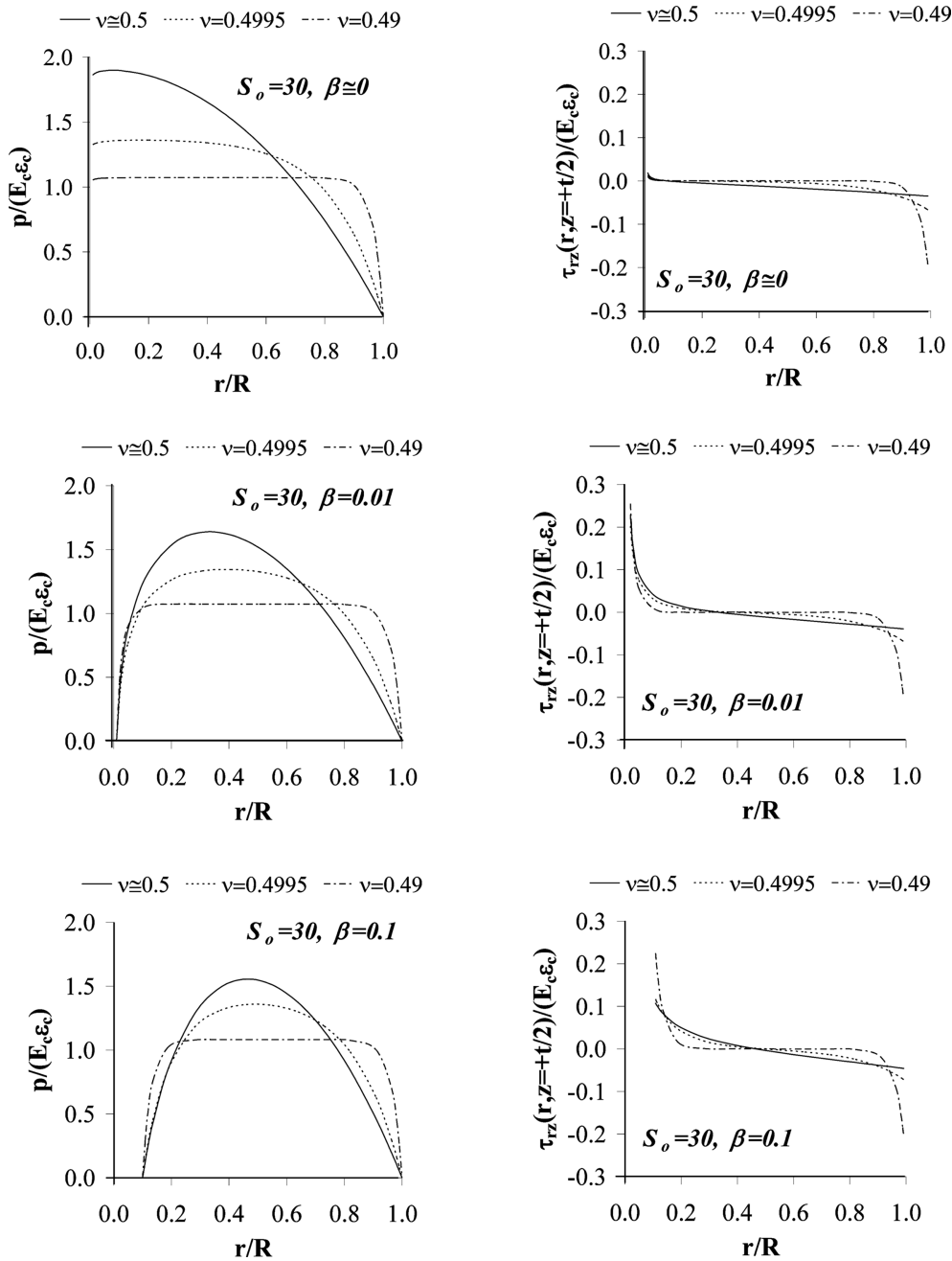

Fig. 9 Effect of the presence of a small to moderate hole on pressure and shear stress distributions for $k_f/Gt = 30000$
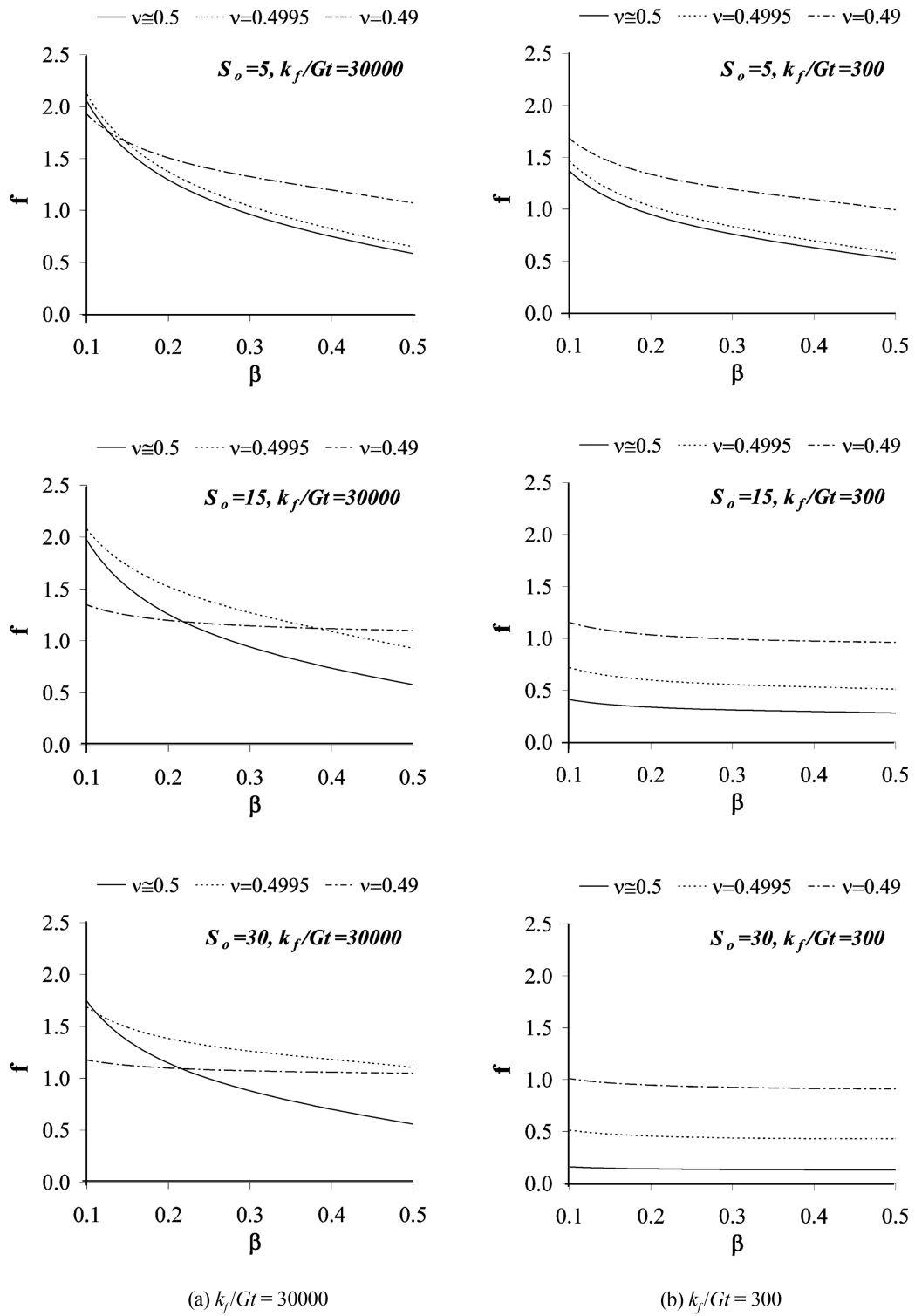
(a) $k_f/Gt = 30000$ (b) $k_f/Gt = 300$

Fig. 10 Magnification factors in practical ranges of parameters

hole ($\beta = 0.01$) are unexpectedly large, particularly if k_f^* is also large. The presence of slight compressibility can decrease these large values significantly in HSF bearings. As β increases, f decreases. The decrease is more significant when $\nu = 0.5$.

Fig. 8 shows how f increases as $\beta \to 0$ and decreases as $\beta \to 1$. The presence of even slight compressibility ($\nu = 0.4995$) can decrease f values considerably when β is small particularly if S_o and k_f^* are large. k_f^* has a similar effect on f. The curves plotted for $k_f^* = 300$ and/or $\nu = 0.49$ are almost uniform, except near $\beta \to 0$. The unexpected behavior observed for very small holes can be explained by plotting the stress distributions, as shown in Fig. 9. Even though the maximum pressure occurs at the center of a circular bearing, the presence of a central hole cause an abrupt decrease in pressure near the hole in a hollow circular bearing. Since shear stress depends on pressure, such a change in pressure distribution also affects shear stress distribution. In fact, as discussed in Pinarbasi *et al.* (2008), the behavior of a hollow circular bearing approaches the behavior of long strip as diameter ratio approaches 1.0. (For more detailed discussions about the stress concentrations near the edges, one may refer to Pinarbasi *et al.* (2008)).

It is also worth noting that in the practical range of $\beta \geq 0.1$ (see Fig. 10), f values are no more than 2.5. It can also be concluded that ignoring the bulk compressibility of rubber may significantly underestimate f unless S_o is low.

4. Conclusions

Due to its favorable mechanical properties, "bonded" rubber layers have long been used in various engineering applications, mostly in the form of multilayered rubber bearings. Until recently, these bearings are usually "reinforced" with steel plates. In an attempt to decrease both the cost and weight of the bearings, Kelly (1999) proposed the use of fiber-reinforcement in place of steel reinforcement. Although the idea is new, the viability of the concept has already been proven by several analytical and experimental studies.

Earlier studies on annular rubber bearings, all of which are conducted for steel-reinforced bearings (to the authors' best knowledge), have indicated that the hole existence not only decreases the compression modulus of the bearing but also increases the maximum shear strain generated in the bearing by compression, both of which are basic design parameters also for fiber-reinforced bearings. Thus, it is essential that the effects of both the hole presence and reinforcement flexibility on the compressive behavior of an annular fiber-reinforced bearing be well understood and properly included in its design.

This paper presents analytical solutions to the problem of uniform compression of hollow-circular fiber-reinforced bearings (HCFRRBs), which includes the solid-circular bearings as a special case as the radius of hollow section vanishes. The problem is handled using the most-recent formulation of the pressure method developed by Kelly (1999), which includes both rubber compressibility and reinforcement flexibility. The analytical solutions are, then, used to investigate the effects of reinforcement flexibility and hole presence on bearing's compression modulus and maximum shear strain developing in the bearing. Main conclusions can be summarized as follows:

- The compressive behavior of an HCFRRB with outer radius R, inner radius a, interior rubber layers of thickness t, shear modulus G and Poisson's ratio ν, interior fiber-reinforcing sheets of thickness t_f and in-plane stiffness $k_f = E_f t_f/(1 - \nu_f^2)$, where E_f and ν_f are, respectively, elasticity modulus and Poisson's ratio of the reinforcing sheet, is controlled by four main parameters: (i)

"stiffness ratio" of the reinforcement $k_f^* = k_f/Gt$, (ii) "radius ratio" of the hole $\beta = a/R$, (iii) Poisson's ratio of rubber ν and (iv) "initial shape factor" of the bearing $S_o = R/2t$.

• The compressive behavior of a HCFRRB asymptotically approaches to that of its corresponding (i.e., with identical S_o, β and ν) steel-reinforced bearing as k_f^* increases. The k_f^* value at which the steel-reinforced behavior is attained decreases as ν and/or S_o decreases and/or β increases.

• The compression modulus of a HCFRRB ($E_{c,HC}$) decreases as β increases. The decrease in $E_{c,HC}$ with increasing β is *not* linear in general. For incompressible materials ($\nu = 0.5$), $E_{c,HC}$ reduces abruptly near $\beta = 0$. The presence of slight compressibility (e.g., $\nu = 0.4995$) decreases this effect noticeably if S_o is high. In the same way, as k_f^* decreases, moderate shape factor (MSF) and high shape factor (HSF) bearings become less sensitive to the hole existence.

• Another important effect of the presence of a central hole in compressive behavior of a circular fiber-reinforced rubber bearing is its increase in bonding shear strain, which is one of the basic design parameters for such bearings. "Magnification factor (f)" can reach very large values when β is considerably small particularly if ν and/or k_f^* are large. As an example, independent of S_o, a hole with $\beta = 0.01$ results in $f \cong 11.0$ when $\nu = 0.5$ and k_f^* is large. The presence of even slight compressibility can decrease this large value considerably in MSF and HSF bearings. When $\beta \geq 0.1$, however, f values are much smaller, no more than 2.5 even for low shape factor (LSF) bearings and/or incompressible cases. The numerical study shows that in this range (i.e., when $\beta \geq 0.1$), ignoring the effects of bulk compressibility of rubber may lead to underestimated magnification factors unless the shape factor of the bearings is small.

• The compressive behavior of a HCFRRB asymptotically approaches to its "incompressible" behavior as bulk compressibility of rubber decreases. The limiting value for ν at which the incompressible bearing behavior is attained decreases as k_f^* decreases and/or S_o decreases and/or β increases. Since LSF bearings reach their incompressible behavior at smaller values of ν, they are *not* influenced from the presence of slight compressibility ($\nu = 0.4995$). For this reason, their compression modulus can be computed from the expressions derived ignoring rubber compressibility. On the other hand, the compressive behavior of an MSF or HSF bearing with slight compressibility can be considerably different than their incompressible behavior particularly if the reinforcement extensibility is small. For this reason, it is essential that the effects of the bulk compressibility of rubber be included in the design of MSF and HSF bearings.

References

Ashkezari, G.D., Aghakouchak, A.A. and Kokabi, M. (2008), "Design, manufacturing and evaluation of the performance of steel like fiber reinforced elastomeric seismic isolators", *J. Mater. Process. Tech.*, **197**(1-3), 140-150.

Gent, A.N. and Lindley, P.B. (1959), "The compression of bonded rubber blocks", *Proc. Inst. Mech. Eng.*, **173**, 111-122.

Kang, G.J. and Kang, B.S. (2009), "Dynamic analysis of fiber-reinforced elastomeric isolation structures", *J. Mech. Sci. Technol.*, **23**(4), 1132-1141.

Kelly, J.M. (1997), *Earthquake Resistant Design with Rubber*, Springer-Verlag, London.

Kelly, J.M. (1999), "Analysis of fiber-reinforced elastomeric isolators", *J. Seismol. Earthq. Eng.*, **2**(1), 19-34.

Kelly, J.M. and Takhirov, S.M. (2001), *Analytical and Experimental Study of Fiber-reinforced Elastomeric Isolators*, PEER Rep. No.2001/11, Pacific Earthquake Engineering Research Center, University of California, Berkeley, California, USA.

Kelly, J.M. and Takhirov, S.M. (2002), *Analytical and Experimental Study of Fiber-reinforced Strip Isolators*, PEER Rep. No.2002/11, Pacific Earthquake Engineering Research Center, University of California, Berkeley, California, USA.

Kelly, J.M. (2002), "Seismic isolation systems for developing countries", *Earthq. Spectra*, **18**(3), 385-406.

Kim, T.H., Kim, Y.J. and Shin, H.M. (2008), "Seismic performance assessment of reinforced concrete bridge piers supported by laminated rubber bearings", *Struct. Eng. Mech.*, **29**(3), 259-278.

Lindley, P.B. (1968), "Effect of Poisson's ratio on compression modulus", *J. Strain. Anal.*, **3**, 142-145.

Lindley, P.B. (1974), *Engineering Design with Natural Rubber*, NR Technical Bulletin, Malaysian Rubber Producers' Research Association, London.

Ling, Y.L., Engel, P.A. and Brodsky, L. (1995), "Compression of bonded annular rubber blocks", *J. Eng. Mech.*, **121**(6), 661-666.

Ling, Y.L. (1996), "An approximate solution for the compression of a bonded thin annular disk", *J. Appl. Mech. ASME*, **63**(3), 780-787.

Mordini, A. and Strauss, A. (2008), "An innovative earthquake isolation system using fibre reinforced rubber rubber bearings", *Eng. Struct.*, **30**(10), 2739-2751.

Naeim, F. and Kelly, J.M. (1999), *Design of Seismic Isolated Structures*, John Wiley & Sons Inc.

Olmos, B.A. and Roesset, J.M. (2010), "Effects of nonlinear behavior of lead-rubber bearings on the seismic response of bridges", *Earthq. Struct.*, **1**(2), 215-230.

Papoulia, K.D. and Kelly, J.M. (1996), "Compression of bonded soft elastic material: variational solution", *J. Eng. Mech.-ASCE*, **122**(2), 163-170.

Pinarbasi, S., Akyuz, U. and Mengi, Y. (2006), "A new formulation for the analysis of elastic layers bonded to rigid surfaces", *Int. J. Solids Struct.*, **43**(14-15), 4271-4296.

Pinarbasi, S. and Mengi, Y. (2008), "Elastic layers bonded to flexible reinforcements", *Int. J. Solids Struct.*, **45**(3-4), 794-820.

Pinarbasi, S., Mengi, Y. and Akyuz, U. (2008), "Compression of solid and annular circular discs bonded to rigid surfaces", *Int. J. Solids Struct.*, **45**(16), 4543-4561.

Toopchi-Nezhad, H., Drysdale, R.G. and Tait, M.J. (2008), "Testing and modeling of square carbon fiber-reinforced elastomeric seismic isolators", *Struct. Control Health Monit.*, **15**(6), 876-900.

Toopchi-Nezhad, H., Drysdale, R.G. and Tait, M.J. (2009), "Parametric study on the response of stable unbonded-fiber reinforced elastomeric isolators (SU-FREIs)", *J. Compos. Mater.*, **43**(15), 1569-1587.

Tsai, H.C. and Lee, C.C. (1998), "Compressive stiffness of elastic layers bonded between rigid plates", *Int. J. Solids Struct.*, **35**(23), 3053-3069.

Tsai, H.C. and Kelly, J.M. (2001), *Stiffness Analysis of Fiber-reinforced Elastomeric Isolators*, PEER Rep. No.2001/05, Pacific Earthquake Engineering Research Center, University of California, Berkeley, California, USA.

Tsai, H.C. and Kelly, J.M. (2005a), "Buckling of short beams with warping effect included", *Int. J. Solids Struct.*, **42**(1), 239-253.

Tsai, H.C. and Kelly, J.M. (2005b), "Buckling load of seismic isolators affected by flexibility of reinforcement", *Int. J. Solids Struct.*, **42**(1), 255-269.

Tsai, H.C. (2006), "Compression stiffness of circular bearings of laminated elastic material interleaving with flexible reinforcements", *Int. J. Solids Struct.*, **43**(11-12), 3484-3497.

Tsai, H.C. (2007), "Tilting analysis of circular elastic layers interleaving with flexible reinforcements", *Int. J. Solids Struct.*, **44**(18-19), 6318-6329.